

Coverage and strain dependent magnetization of titanium-coated carbon nanotubes

S. Dag and S. Ciraci*

Department of Physics, Bilkent University, Ankara 06800, Turkey

(Received 8 December 2004; published 12 April 2005)

First-principles, spin-relaxed pseudopotential plane wave calculations show that Ti atoms can form a continuous coating of carbon nanotubes at different amounts of coverage. Fully relaxed geometry has a complex but regular atomic structure. The semiconducting tube becomes ferromagnetic metal with high quantum conductance. However, the magnetic properties of Ti-coated tubes depend strongly on the geometry, amount of Ti coverage and also on the elastic deformation of the tube. While the magnetic moment can be pronounced significantly by the positive axial strain, it can decrease dramatically upon the adsorption of additional Ti atoms to those already covering the nanotube. Besides, the electronic structure and the spin-polarization near the Fermi level can also be modified by radial strain.

DOI: 10.1103/PhysRevB.71.165414

PACS number(s): 73.22.-f, 61.48.+c, 73.20.Hb, 71.30.+h

I. INTRODUCTION

Continuous Ti coating of varying thickness, and quasicontinuous Ni and Pd coating of single-wall carbon nanotubes (SWNT) have been obtained by using electron beam evaporation techniques.¹ Calculations have provided theoretical support for those experimental findings showing that SWNTs can be covered continuously by Ti atoms^{2,3} and form a complex but regular atomic structure with a squarelike cross section.⁴ Upon Ti coating, a semiconducting SWNT (s-SWNT) becomes metallic with high density of states (DOS) at the Fermi level, $D(E_F)$, and high quantum conductance. More importantly, Ti-coated SWNTs have ferromagnetic ground states with large magnetic moments μ .⁴ While metal-coated SWNTs with a controllable size and high conductance have been considered very promising as interconnects in future nanoelectronics, nanostructures, or nanowires having ferromagnetic ground states and large spin polarizations at the Fermi energy E_F have been a subject of interest in spintronics.^{4,5}

Spintronics aims to increase the information transport capacity and versatility of electronic devices by using the spin degrees of freedom of conduction electrons.⁶⁻¹⁰ Owing to the broken spin degeneracy in a magnetic ground state, energy bands $E_n(\mathbf{k}\uparrow)$ and $E_n(\mathbf{k}\downarrow)$ split, and may lead to different density of states for different spin orientations. In this paper, we elucidate our findings reported earlier as a short communication⁴ by placing emphasis on the electronic structure of a Ti-coated SWNT corresponding to its ferromagnetic ground state, and by further investigating its spin-dependent properties. We, in particular, are concerned with the spin polarization at E_F ,

$$P(E_F) = \frac{|D^\uparrow(E_F) - D^\downarrow(E_F)|}{D^\uparrow(E_F) + D^\downarrow(E_F)}, \quad (1)$$

in terms of majority (minority) spin density of states $D^\uparrow(E_F)$ [$D^\downarrow(E_F)$]. We investigate how the magnetic moment μ , and $P(E_F)$ can be modified with the applied strain and amount of Ti coverage. We found that μ , as well as $P(E_F)$, depends strongly on the applied strain and on the Ti coverage. While a strain of $\epsilon_{zz}=0.1$ along the axis of the tube induces a 25% increase of μ , the adsorption of four addi-

tional Ti atoms on the Ti-coated (8,0) SWNT causes a 44% reduction of the magnetic moment. The radial strain leading to the elliptical deformation of the circular cross section modifies the spin-dependent electronic structure near E_F . The manipulation of the spin-dependent properties of a Ti-coated SWNT with applied strain and with Ti coverage suggest interesting technological applications such as spin filters, spin-resonant tunneling diodes, unipolar spin transistors, and nanoscale magnetism, etc.

II. METHOD

We performed spin-relaxed, first-principles pseudopotential plane wave calculations^{11,12} within the density functional theory.¹³ We used a spin-polarized generalized gradient approximation¹⁴ (GGSA) and ultrasoft pseudopotential^{12,15} with a uniform energy cutoff of 300 eV. Calculations have been performed in momentum space by using periodically repeating tetragonal supercells with lattice constants, $a_s=b_s \sim 20 \text{ \AA}$ and $c_s=c$ [c being the one-dimensional (1D) lattice constant of SWNT]. The Brillouin zone of the supercell is sampled by using the Monkhorst-Pack¹⁶ special \mathbf{k} -point scheme. All atomic positions (i.e., all adsorbed Ti atoms and carbon atoms of a SWNT), as well as c_s , have been optimized. In order to further test that the structures of Ti-adsorbed or Ti-coated SWNTs obtained through geometry optimization are stable, we carried out *ab-initio* molecular dynamics calculations at $T=500 \text{ K}$ using the Nosé thermostat. All structures reported in this paper are maintained stable at $T=500 \text{ K}$ for a sufficient number of time steps.

III. RESULTS AND DISCUSSION

Adsorption of an individual Ti atom above the center of hexagon (i.e., H site) is found to be energetically most favorable; it has a binding energy of $E_b=2.2 \text{ eV}$ and a magnetic moment of $\mu=2.2 \mu_B$ (Bohr magneton) in the magnetic ground state.² Ti $3d$ orbitals play a crucial role in the bonding, and electrons are transferred from Ti to SWNT.^{2,3} Significant adsorption energy of $E_b=2.2 \text{ eV}$ indicates a rather strong Ti-SWNT chemisorption bond formed by charge rearrangement between Ti and C atoms. This way, one of the

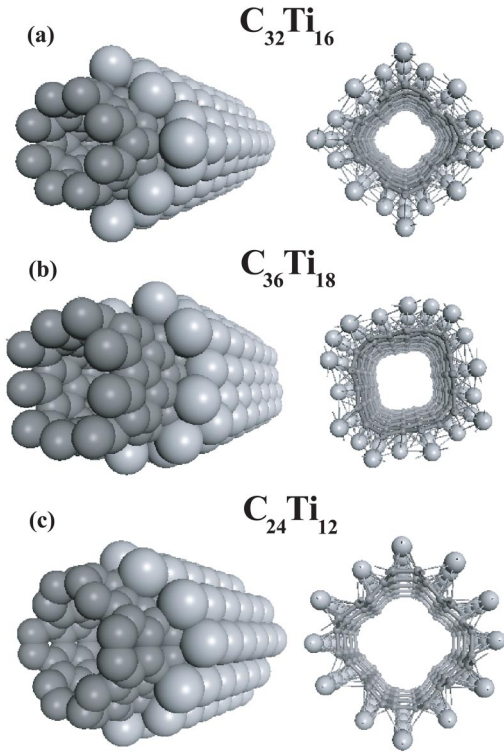


FIG. 1. Optimized atomic structures of Ti-covered (a) (8,0) SWNT ($C_{32}Ti_{16}$); (b) (9,0) SWNT ($C_{36}Ti_{18}$); (c) (6,6) SWNT ($C_{24}Ti_{12}$).

necessary conditions needed to form a continuous metal coverage has been met.

The Ti coverage of (8,0) SWNT has been analyzed first by attaching Ti atoms at all H sites in the unit cell, and subsequently by optimizing the atomic structure.⁴ Here, we examine the role of coupling among adsorbates, which becomes pronounced by the increasing number of adsorbed Ti atoms. The Ti-Ti coupling is the prime interaction favoring cluster formation, but endangering the continuous coating of the SWNT. The relaxation of the SWNT lattice has been found to be crucial in obtaining stable structures; the frozen lattice constant has led to instabilities. The average binding energy, of the Ti-coated (8,0) SWNT described in Fig. 1(a) (which is specified as $C_{32}Ti_{16}$),

$$\bar{E}_b = \{16E_T[\text{Ti}] + E_T[\text{SWNT}] - E_T[\text{Ti} + \text{SWNT}]\}/16, \quad (2)$$

has been found (in terms of the total energies of individual Ti atoms, optimized bare SWNTs, and Ti-covered SWNTs) to be 4.3 eV for the equilibrium lattice parameter $c=c_0$. Because of the attractive interaction among nearest-neighbor Ti atoms, \bar{E}_b comes out much higher than the binding energy of the adsorbed single Ti atom. The charge transferred from Ti to C is approximately 0.4 electrons in the case of continuous coating, $C_{32}Ti_{16}$. This value is about 0.6 electrons smaller than the charge transferred from a single Ti atom adsorbed on an (8,0) SWNT. It appears that the interaction between individual Ti and a SWNT is decreased by the Ti-Ti coupling, causing a back transfer of the charge. Nevertheless, for

a uniform coating, the Ti-C interaction has to overcome the Ti-Ti interaction. Otherwise, adsorbed Ti atoms would be clustered to form small Ti particles on the surface of the SWNT so that continuous coating would be hampered as one experienced for other adsorbed transition metal atoms. A significant C-Ti interaction occurs through Ti-3*d* and C-2*p* hybridization; it is comparable to Ti-Ti coupling and is almost unique to Ti among transition metal elements. This makes Ti an important element in the coating of SWNTs.¹ Depending on the radius and chirality, the circular cross section changes to either a squarelike or polygonal form as described in Fig. 1.⁴ The magnetic moments were calculated at 15.3, 13.7, and 9.5 μ_B for Ti-coated (8,0) (i.e., $C_{32}Ti_{16}$), (9,0) (i.e., $C_{36}Ti_{18}$), and (6,6) ($C_{24}Ti_{12}$) SWNTs, respectively. While spin-unpolarized band structure calculations⁴ have indicated that these systems are quasi-one-dimensional metals¹⁷ with high DOS at E_F , spin-polarized bands corresponding to the ferromagnetic ground state have been studied in the present paper.

We investigate now the effect of the adsorption of additional Ti atoms on the $C_{32}Ti_{16}$ surface. Whether the regular atomic structure and the electronic properties of $C_{32}Ti_{16}$ are affected will be the issue we shall clarify. To this end, we consider that four additional Ti atoms are attached at the corners of the squarelike cross section of $C_{32}Ti_{16}$ to make $C_{32}Ti_{20}$. The fully optimized, stable atomic structure of $C_{32}Ti_{20}$ is shown in Fig. 2(d). The adsorption of four additional Ti atoms corresponds to the initial stage of a second Ti atomic layer to cover the SWNT surface. The average binding energy of these additional Ti atoms was found to be ~ 4.6 eV/atom. It is larger than that of $C_{32}Ti_{16}$, owing to the onset of the Ti-Ti coupling in three dimensions. The effect of these four Ti atoms on the structure of $C_{32}Ti_{16}$ is minute. However, the calculated magnetic moment undergoes a dramatic change upon the chemisorption; μ of $C_{32}Ti_{16}$ decreases from 15.3 to 6.8 μ_B /cell in $C_{32}Ti_{20}$. This important result implies that the net magnetic moment of a Ti-covered SWNT is strongly dependent on the amount, as well as geometry, of Ti coverage. The magnetization of the nanostructure $C_{4n}Ti_N$ can be engineered by varying the number N , and the decoration of adsorbed Ti atoms.

Next, we examine the effect of Ti coverage on the spin-dependent electronic properties. The spin-polarized energy band structure and densities of states for majority and minority spin states of the Ti-coated (8,0) SWNT are presented in Fig. 2. The band structure of the bare (8,0) sSWNT has changed dramatically; the band gap between conduction and valence band diminished because of several bands crossing the Fermi level. The total current in magnetic systems can be obtained as $I = I^\uparrow + I^\downarrow$, where I^\uparrow (I^\downarrow) is the contribution to the current from majority (minority) spin-current-carrying states. The current for a given spin orientation is obtained using the Landauer formula¹⁷⁻¹⁹

$$I^{\uparrow(\downarrow)}(V_b) = \frac{e^2}{h} \int_{\mu_L}^{\mu_R} dE (f_L - f_R) T^{\uparrow(\downarrow)}(E, V_b) \quad (3)$$

in terms of the bias voltage V_b ; the Fermi distribution function of left and right electrodes f_L and f_R , and their chemical potentials μ_L and μ_R . $T^{\uparrow(\downarrow)}(E, V_b)$ is the transmission func-

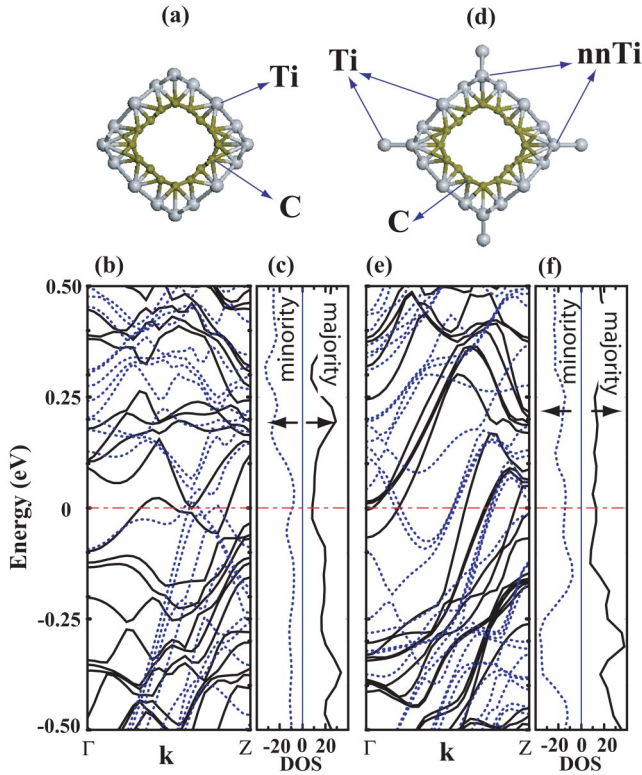


FIG. 2. (Color online) (a) Fully optimized atomic structure and squarelike cross section of Ti-coated (8,0) zigzag SWNT including 16 Ti atoms per unit cell ($C_{32}Ti_{16}$). Ti and C atoms are indicated by large-light and small-dark circles. (b) The spin-polarized band structure of $C_{32}Ti_{16}$ at $\epsilon_{zz}=0$ with the Fermi level set to zero of energy. Majority spin, $E_n(\mathbf{k}\uparrow)$ and minority spin, $E_n(\mathbf{k}\downarrow)$ bands are shown by continuous and dotted lines, respectively. The spin-polarized density of states for the majority $D^\uparrow(E)$ and minority $D^\downarrow(E)$ spin states. (d) The fully optimized atomic structure of a Ti-coated (8,0) SWNT including four additional Ti atoms adsorbed at the corners of the squarelike tube (i.e., $C_{32}Ti_{20}$). (e) and (d) show the corresponding spin-polarized band structure and DOS, respectively. The nearest Ti atoms to the four additional adsorbed Ti atoms are indicated by nnTi.

tion for the majority or spin-up (spin-down) electrons calculated using the Green's function approach. $\mathcal{T}^{\uparrow(\downarrow)}(E, V_b)$ is reduced due to the scattering of carriers from the abrupt change of cross sections, irregularities at the contacts to electrodes, and also from the imperfections, impurities, and electron-phonon interaction in the tube by itself. In a self-consistent treatment, the contact potential also causes \mathcal{T} to decrease. Therefore, a rigorous treatment of the conductance of a finite-size Ti-coated SWNT (device) requires a detailed description of electrodes and the contact structure. In the above expression the mixing of spin channels, namely the spin flip from one orientation to the other, is not allowed. In reality, owing to the coupling with phonons, the spin flip can take place. Here, since we are concerned with transport properties of nanowire rather than with a particular device, we infer G from an ideal Ti-coated SWNT. Under these circumstances, the mean free path of electrons l_m becomes infinite at $T=0$, and the electronic transport occurs ballistically and coherently. This situation has been treated as an ideal 1D

constriction, where the electrons are confined in the transversal direction, but propagate freely along the axis of the wire.¹⁷ Then the current, for example, for majority spin states can be expressed as $I^\uparrow = \sum_i \eta_i^\uparrow e v_i^\uparrow [D_i^\uparrow(E_F + eV_b) - D_i^\uparrow(E_F)]$, where degeneracy, group velocity, and density of states of each subband crossing E_F for spin-up electrons are given by η_i^\uparrow , v_i^\uparrow , D_i^\uparrow , respectively. Since $D_i^\uparrow(E_F + eV_b) - D_i^\uparrow(E_F) \sim (eV_b) \partial D_i^\uparrow(E) / \partial E|_{E_F}$ and $1/v_i^\uparrow = \hbar \partial D_i^\uparrow / \partial E|_{E_F}$, then $G^\uparrow = I^\uparrow / V_b = \sum_i \eta_i^\uparrow e^2 / h$. Accordingly each subband crossing the Fermi level is counted as $\eta_i^{\uparrow(\downarrow)}$ current-carrying state for a given spin direction with channel transmission $\mathcal{T}^{\uparrow(\downarrow)} = 1$. Then the maximum ‘‘ideal’’ conductance of a defect-free Ti-covered ideal tube becomes $G^{\uparrow(\downarrow)} = e^2 N_b^{\uparrow(\downarrow)} / h$, where $N_b^{\uparrow(\downarrow)} = \sum_i \eta_i^{\uparrow(\downarrow)}$. We found $G^\uparrow = 4e^2/h$, $G^\downarrow = 5e^2/h$ for $C_{32}Ti_{16}$ and $G^\uparrow = 6e^2/h$, $G^\downarrow = 8e^2/h$ for $C_{32}Ti_{20}$. Apparently, more bands that cross the Fermi level increase $D^\uparrow(E_F)$ and $D^\downarrow(E_F)$ upon the adsorption of the additional four Ti atoms.

We note that the regular structure shown in Fig. 2 may occur under idealized conditions; normally irregularities are unavoidable, in particular for a thick Ti coating. While the transmission coefficient can decrease in the thick but inhomogeneous Ti coating, G is expected to be still high owing to the new conductance channels opened at E_F .

Densities of states corresponding to majority and minority spin states in Fig. 2 indicate that $P(E_F)$ is low and hence $C_{32}Ti_{16}$ and $C_{32}Ti_{20}$ structures, apart from being high conducting, may not be of interest for spintronics applications. Present results indicate that the spin-dependent electronic structure and the magnetic moment of these nanostructures can be modified also by applied axial and radial strain, ϵ_{zz} . In Fig. 3(a) the magnetization of a Ti-covered (8,0) SWNT is plotted as a function of c . Each theoretical data point corresponds to the magnetic moment of $C_{32}Ti_{16}$ system relaxed under the constraint of a fixed c , hence under a given axial strain ϵ_{zz} . Figures 3(b) and 3(c) also show the change of stress and total energy as a function of c . The equilibrium lattice parameter occurs at $c_0 = 4.17 \text{ \AA}$. The axial strain is defined as $\epsilon_{zz} = (c - c_0) / c$. Starting from a compressive range with $\epsilon_{zz} < 0$, the net magnetic moment μ of $C_{32}Ti_{16}$ increases with increasing c , and continues to increase by stretching the system along the tube axis in the tensile range with $\epsilon_{zz} > 0$.

Ferromagnetism in magnetic structures is generally explained in terms of the Heisenberg model, which considers spin-spin coupling between magnetic atoms at different lattice sites through exchange interaction. First-principles calculations based on the discrete Fourier transform (DFT), which treat the magnetism of metallic structures from the viewpoint of itinerant electrons, reveal that a ferromagnetic state is energetically favorable. In fact, when c increases, the average Ti-Ti distance will increase (see inset in Fig. 3). Here parallel spin alignment is promoted by a p - d hybridization, hence by electron transfer between the localized d orbitals of Ti atoms and extended $2p$ orbitals of C atoms. The important role of C atoms is also pointed out in recent DFT calculations,² where p orbitals of C are found to interact strongly with the d orbitals of adsorbed Ti. The stronger the p - d hybridization, the lower the d - d exchange interaction and so as the resulting magnetic moment. Here, increasing

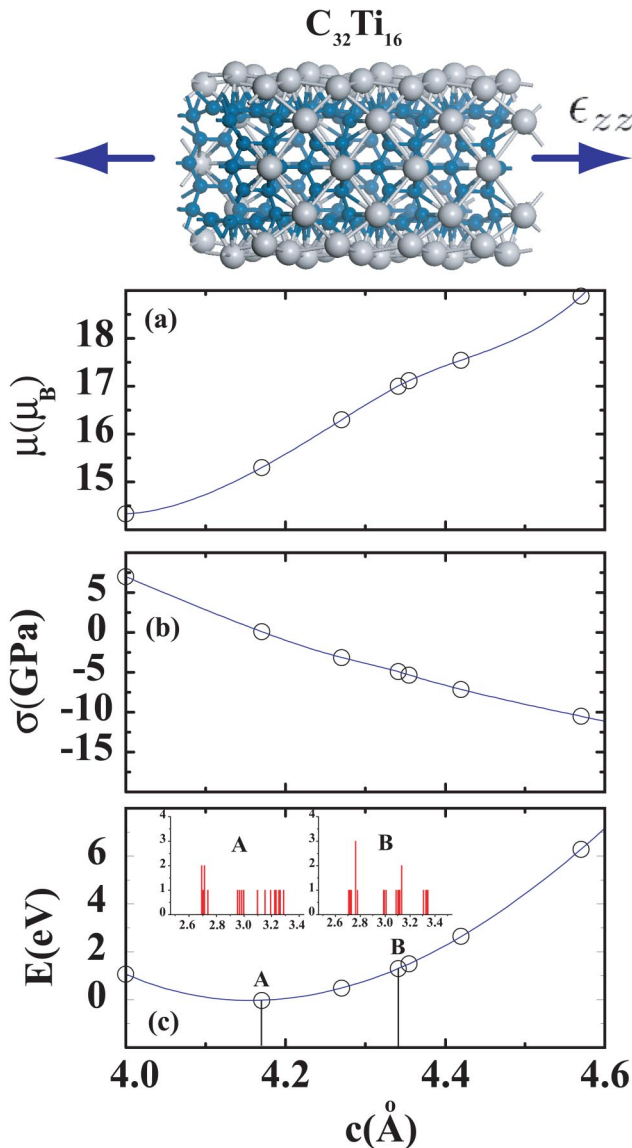


FIG. 3. (Color online) Top inset: a side view of the Ti-covered (8,0) SWNT (i.e., $C_{32}Ti_{16}$) strained along its axis. $\epsilon_{zz} > 0$ corresponds to the stretched structure with $c > c_0$. (a) A variation of the magnetic moment μ per unit cell of $C_{32}Ti_{16}$ as a function of the lattice parameter c or strain. (b) The calculated axial stress in the system as a function of c . (c) A variation of the total energy E with c . The minimum of E occurs at $c_0 = 4.17$ \AA . The insets in (c) show the distribution of Ti-Ti bond lengths corresponding to $c_0 = 4.17$ \AA and $c = 4.34$ \AA .

the Ti-Ti distance decreases the d - d coupling between Ti-Ti atoms, but increases the p - d hybridization. The fact that in the absence of Ti-Ti coupling the magnetic moment of $C_{32}Ti_{16}$ could be 16 times the magnetic moment of $C_{32}Ti$, i.e., $16 \times 2.2 \mu_B$ instead of $15.3 \mu_B$, corroborates our arguments.

The decrease of the magnetic moment of $C_{32}Ti_{16}$ from 15.3 to $6.8 \mu_B$ owing to the adsorption of four additional Ti atoms can be explained also by using similar arguments. In Fig. 2(d), additional Ti atoms adsorbed at the high curvature sites of squarelike cross sections of $C_{32}Ti_{16}$ affect the inter-

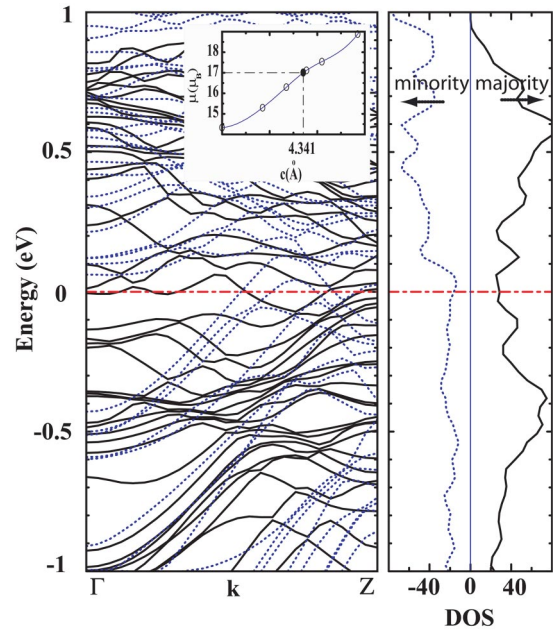


FIG. 4. (Color online) Calculated spin-polarized band structure of $C_{32}Ti_{16}$ under $\epsilon_{zz} = 0.04$ at $c = 4.34$ \AA . $E_n(\mathbf{k}\uparrow)$ and $E_n(\mathbf{k}\downarrow)$ are shown by continuous and dotted lines, respectively. The corresponding densities of the majority and minority spin states are shown in the panel on the right-hand side.

action between existing Ti atoms at their close proximity with the nearest C atoms of the SWNT. These Ti atoms are specified as nnTi atoms in Fig. 2(d). Increasing coupling among Ti atoms by forming three-dimensional-like Ti particles at the corners causes an electronic charge that was donated to nearby C atoms to be back donated to nnTi atoms and hence to decrease the p - d hybridization. A detailed charge density analysis shows that the excess charge of ~ 0.3 electrons at each carbon atom interacting with nnTi atoms of $C_{32}Ti_{20}$ decreases to ~ 0.2 electrons upon the adsorption of four additional Ti atoms. At the end, nnTi atoms, which initially carry majority spin as others, have their spin flipped upon the adsorption of additional Ti atoms. This situation implies that the magnetic moment of the Ti-coated SWNT will decrease further as Ti coverage increases.

Half-metals⁸⁻¹⁰ are another class of materials that exhibit spin-dependent electronic properties relevant for spintronics. Half-metals, where the bands exhibit metallic behavior for one spin direction but become semiconducting for the opposite spin direction, provide the ultimate spin polarization of $P = 1$ at E_F . Accordingly, the difference between the majority and minority spin electrons per unit cell should be an integer number. Interestingly, as seen in Fig. 3(a) the magnetic moment of $C_{32}Ti_{16}$ becomes equal to $17 \mu_B$ under the strain $\epsilon_{zz} \sim 0.04$ corresponding to $c = 4.34$ \AA . An integer μ per unit cell reminds of the possibility of a half-metallic behavior. In Fig. 4 the band structure and DOS of $C_{32}Ti_{16}$ corresponding to $\epsilon_{zz} \sim 0.04$ are illustrated. Here, since both $E_n(\mathbf{k}\uparrow)$ and $E_n(\mathbf{k}\downarrow)$ cross the Fermi level, the system is a ferromagnetic metal, but $P(E_F)$ is significantly increased as compared to the case of $\epsilon_{zz} = 0$ [shown in Fig. 2(b)]. Hence, whereas the half-metallic behavior did not occur, the spin polarization has

been enhanced significantly and becomes suitable for spintronic applications. The analysis of spin-polarized bands of $C_{32}Ti_{16}$ for $c_0=4.17 \text{ \AA}$ and $c=4.34 \text{ \AA}$ shows that in the latter 64% (36%) of the current is carried by majority (minority) spin states. Whereas, in the case of $c_0=4.17 \text{ \AA}$ (i.e., $\epsilon_{zz}=0$) the shares of majority and minority spins are almost equal. This is clearly another interesting effect of applied strain.

Finally, we explore the effect of radial strain $\epsilon_{yy}=(b-R)/R$, which is defined in terms of the minor, b , and major, a , axes of the elliptically deformed cross section and the radius R of the bare tube. Earlier studies have revealed important effects of the radial deformation of SWNTs on their electronic and chemical properties.^{20,21} For example, a sSWNT has become metallic, and the electronic charge distribution on its surface has undergone a significant change. It has been also found that the chemical activity of SWNT at the high curvature site has increased to lead to a stronger bonding with foreign atoms such as H, Al.²² Here we expect that the spin-dependent electronic structure of Ti adsorbed on the SWNT is affected by radial deformation. In Fig. 5, we show the calculated $D^\uparrow(E)$ and $D^\downarrow(E)$ of the $C_{32}Ti$, where Ti is adsorbed on the bare, as well as at the high curvature site of a radially deformed ($\epsilon_{yy} \sim 0.3$) (8,0) SWNT. Radial deformation had a minute effect on the value of the net magnetic moment. However, the dispersion of bands and $P(E)$ near E_F have been affected by radial deformation. The forms of $D^\uparrow(E)$ and $D^\downarrow(E)$ near E_F suggest that the spin-dependent transport under bias voltage V_b can be monitored by ϵ_{yy} .

IV. CONCLUSION

First-principles spin-relaxed calculations showed that the chemical interaction between SWNTs and the Ti atom adsorbed to the hollow site is significant and favors the continuous coating of the tube surface. A semiconducting SWNT is metallized upon the adsorption of Ti atoms. Zigzag, as well as armchair, SWNTs are metallic and have a ferromagnetic ground state when they are continuously covered with Ti atoms. Spin-relaxed calculations predict interesting spin-dependent electronic and magnetic properties. The magnetic moment of the (8,0) SWNT can increase with the increasing number of adsorbed Ti atoms to a value as large as $15.3 \mu_B$; it, however, decreases if additional Ti atoms are adsorbed on the Ti coating on SWNT surface. On the other hand, electronic conduction channels for each spin direction undergo a change; while $G^\uparrow=4e^2/h$ ($G^\downarrow=5e^2/h$) for $C_{32}Ti_{16}$, it changes to $G^\uparrow=6e^2/h$ ($G^\downarrow=8e^2/h$) for $C_{32}Ti_{20}$. We showed that the magnetic properties of the Ti-covered SWNT can be modified also by applied axial strain; the magnetic moment increases with increasing ϵ_{zz} (namely by stretching the tube). Not only the net magnetic moment, but also the spin polarization at the Fermi level can be increased by increasing axial strain. Finally, we studied the effect of the radial strain on the spin-dependent electronic and magnetic properties.

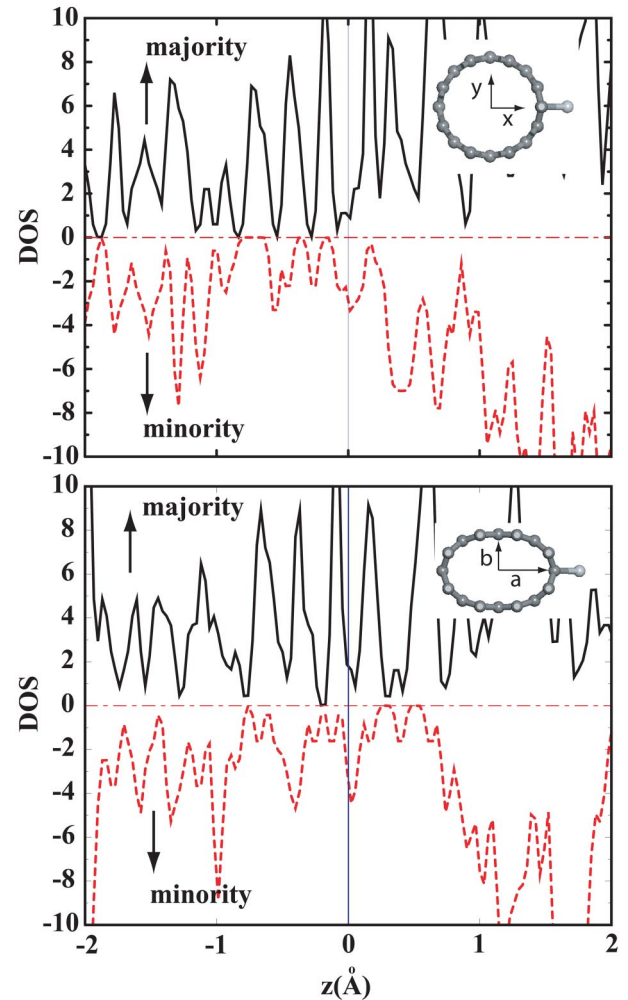


FIG. 5. (Color online) Densities of majority and minority spin states of $C_{32}Ti$ showing the curvature effect on $P(E)$. (a) The density of spin states for a single Ti atom adsorbed on a bare (8,0) SWNT. (b) The density of states for a single Ti atom adsorbed on the high curvature site of an (8,0) SWNT under radial deformation $\epsilon_{yy}=0.3$, which transforms the circular cross section to an elliptical one as shown by the insets.

We found the dispersion of the spin-dependent bands and resulting density of states near the Fermi level of a single Ti-atom-adsorbed (8,0) SWNT is modified upon radial deformation. We expect that these coverage- and strain-dependent electronic and magnetic properties of Ti-coated SWNTs can lead to interesting applications in spintronics and nanoscale magnetism.

ACKNOWLEDGMENTS

S.C. acknowledges the partial support of TUBA, the Academy of Science of Turkey.

*Electronic address: ciraci@fen.bilkent.edu.tr

- ¹Y. Zhang and H. Dai, Appl. Phys. Lett. **77**, 3015 (2000); Y. Zhang, N. W. Franklin, R. J. Chen, and H. Dai, Chem. Phys. Lett. **331**, 35 (2000).
- ²E. Durgun, S. Dag, V. K. Bagci, O. Gülseren, T. Yildirim, and S. Ciraci, Phys. Rev. B **67**, 201401 (2003); E. Durgun, S. Dag, S. Ciraci, and O. Gülseren, J. Phys. Chem. B **108**, 575 (2004).
- ³C.-K. Yang, J. Zhao, and J. P. Lu, Phys. Rev. B **66**, 041403 (2002).
- ⁴S. Dag, E. Durgun, and S. Ciraci, Phys. Rev. B **69**, 121407(R) (2004).
- ⁵C.-K. Yang, J. Zhao, and J. P. Lu, Phys. Rev. Lett. **90**, 257203 (2003).
- ⁶G. A. Prinz, Science **282**, 1660 (1998).
- ⁷P. Ball, Nature (London) **404**, 918 (2000).
- ⁸S. A. Wolf, D. D. Awschalom, R. A. Buhrman, J. M. Daughton, S. von Molnár, M. L. Roukes, A. Y. Chtchelkanova, and D. M. Treger, Science **294**, 1488 (2001).
- ⁹R. A. de Groot, F. M. Mueller, P. G. van Engen, and K. H. J. Bushkow, Phys. Rev. Lett. **50**, 2024 (1983).
- ¹⁰W. E. Pickett, and J. S. Moodera, Phys. Today **54** (5), 39 (2001).
- ¹¹M. C. Payne, M. P. Teter, D. C. Allen, T. A. Arias, and J. D. Joannopoulos, Rev. Mod. Phys. **64**, 1045 (1992).
- ¹²Numerical calculations have been performed by using the VASP package; G. Kresse and J. Hafner, Phys. Rev. B **47**, 558 (1993); G. Kresse and J. Furthmüller, *ibid.* **54**, 11 169 (1996).
- ¹³P. Hohenberg and W. Kohn, Phys. Rev. **136**, B864 (1964); W. Kohn and L. J. Sham, Phys. Rev. **140**, A1133 (1965).
- ¹⁴J. P. Perdew, J. A. Chevary, S. H. Vosko, K. A. Jackson, M. R. Pederson, D. J. Singh, and C. Fiolhais, Phys. Rev. B **46**, 6671 (1992).
- ¹⁵D. Vanderbilt, Phys. Rev. B **41**, 7892 (1990).
- ¹⁶H. J. Monkhorst and J. D. Pack, Phys. Rev. B **13**, 5188 (1976).
- ¹⁷S. Ciraci, A. Buldum, and I. P. Batra, J. Phys.: Condens. Matter **13**, R537 (2001).
- ¹⁸R. Landauer, Z. Phys. B: Condens. Matter **68**, 217 (1987); R. Landauer, Phys. Lett. **85A**, 91 (1981); C. C. Kaun, B. Larade, H. Mehrez, J. Taylor, and H. Guo, Phys. Rev. B **65**, 205416 (2002).
- ¹⁹S. Datta, *Electron Transport in Mesoscopic Systems* (Cambridge University Press, Cambridge, 1997).
- ²⁰S. Ciraci, S. Dag, T. Yildirim, O. Gülseren, and T. Senger, J. Phys.: Condens. Matter **16**, R901 (2004).
- ²¹C. Kilic, S. Ciraci, O. Gülseren, and T. Yildirim, Phys. Rev. B **62**, R16 345 (2000).
- ²²O. Gülseren, T. Yildirim, and S. Ciraci, Phys. Rev. Lett. **87**, 116802 (2001).